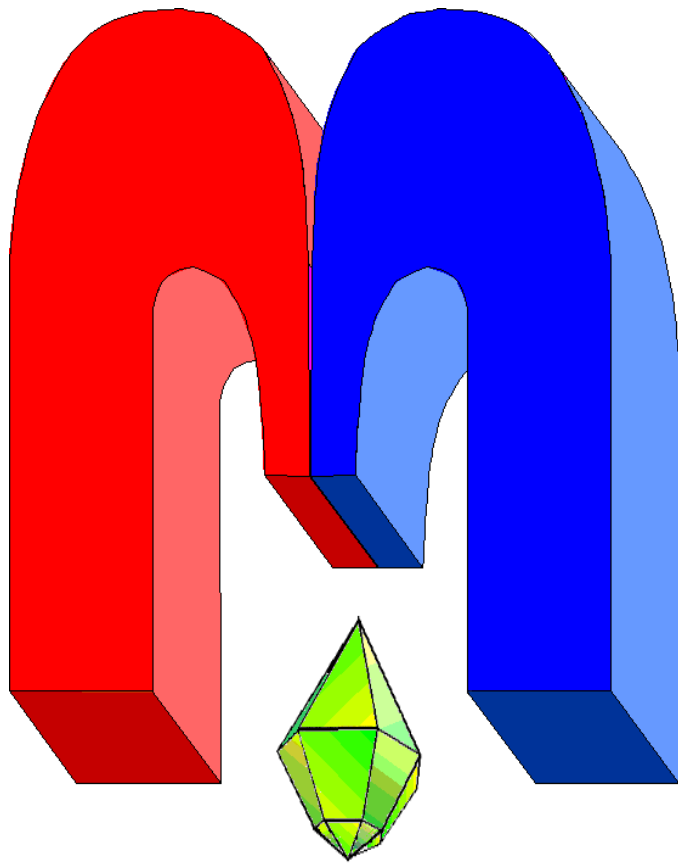


ISSN 2072-5981

doi: 10.26907/mrsej



***magnetic
Resonance
in Solids***

Electronic Journal

Volume 21

Special Issue 4

Paper No 19414

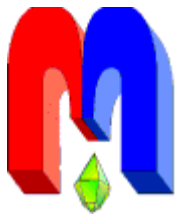
1-7 pages

2019

doi: 10.26907/mrsej-19414

<http://mrsej.kpfu.ru>

<http://mrsej.ksu.ru>



Established and published by Kazan University
Endorsed by International Society of Magnetic Resonance (ISMAR)
Registered by Russian Federation Committee on Press (#015140),
August 2, 1996
First Issue appeared on July 25, 1997

© Kazan Federal University (KFU)*

"Magnetic Resonance in Solids. Electronic Journal" (MRSej) is a peer-reviewed, all electronic journal, publishing articles which meet the highest standards of scientific quality in the field of basic research of a magnetic resonance in solids and related phenomena.

Indexed and abstracted by
Web of Science (ESCI, Clarivate Analytics, from 2015), Scopus (Elsevier, from 2012), RusIndexSC (eLibrary, from 2006), Google Scholar, DOAJ, ROAD, CyberLeninka (from 2006), SCImago Journal & Country Rank, etc.

Editor-in-Chief

Boris **Kochelaev** (KFU, Kazan)

Honorary Editors

Jean **Jeener** (Universite Libre de Bruxelles, Brussels)

Raymond **Orbach** (University of California, Riverside)

Executive Editor

Yurii **Proshin** (KFU, Kazan)
mrsej@kpfu.ru



This work is licensed under a [Creative Commons Attribution-ShareAlike 4.0 International License](https://creativecommons.org/licenses/by-sa/4.0/).



This is an open access journal which means that all content is freely available without charge to the user or his/her institution. This is in accordance with the [BOAI definition of open access](#).

Special Editor of Issue

Eduard **Baibekov** (KFU)

Editors

Vadim **Atsarkin** (Institute of Radio Engineering and Electronics, Moscow)

Yurij **Bunkov** (CNRS, Grenoble)

Mikhail **Eremin** (KFU, Kazan)

David **Fushman** (University of Maryland, College Park)

Hugo **Keller** (University of Zürich, Zürich)

Yoshio **Kitaoka** (Osaka University, Osaka)

Boris **Malkin** (KFU, Kazan)

Alexander **Shengelaya** (Tbilisi State University, Tbilisi)

Jörg **Sichelschmidt** (Max Planck Institute for Chemical Physics of Solids, Dresden)

Haruhiko **Suzuki** (Kanazawa University, Kanazawa)

Murat **Tagirov** (KFU, Kazan)

Dmitrii **Tayurskii** (KFU, Kazan)

Valentine **Zhikharev** (KNRTU, Kazan)

Technical Editors of Issue

Nurbulat **Abishev** (KFU)

Maxim **Avdeev** (KFU)

Eduard **Baibekov** (KFU)

Alexander **Kutuzov** (KFU)

* In Kazan University the Electron Paramagnetic Resonance (EPR) was discovered by Zavoisky E.K. in 1944.

Quantum cellular automata: theoretical study of bistable cells for molecular computing

B. Tsukerblat^{1,2,*}, A. Pali^{3,4}, A. Rybakov^{4,5}

¹Department of Chemistry, Ben-Gurion University of the Negev, Beer-Sheva, Israel

²Ariel University, Ariel, Israel

³Institute of Problems of Chemical Physics, Chernogolovka, Moscow Region, Russia

⁴Institute of Applied Physics, Academy of Sciences of Moldova, Chisinau, Moldova

⁵Moscow Institute of Physics and Technology, Dolgoprudny, Moscow Region, Russia

*E-mail: tsuker@bgu.ac.il

(Received May 24, 2019; accepted May 28, 2019; published June 6, 2019)

The article is devoted to the theoretical study of the four-site cells as the basic units in the architecture of quantum-dot or molecular cellular automata. The functional characteristics of two possible compositions of square cells for quantum cellular automata are compared. We analyze the properties of the tetrameric cells composed of two isolated one-electron dimers (half-cells) and the cells based on the bi-electron tetramers (full cells). The inter-site Coulomb interactions and the electron transfer processes are taken into account as well as the external field of the neighboring cell. The difference in the transfer pathways is shown to result in a more abrupt nonlinear cell-cell response function for the double-dimer arrangement of the charge containers. This result shows that the double-dimeric cell is preferable to design quantum cellular automata devices.

PACS: 31.15.Rh, 31.15.ap, 33.15.-e, 36.40.-c.

Keywords: quantum cellular automata, mixed-valence clusters, cell-cell response, Hubbard Hamiltonian.

*Dedicated to outstanding scientist and dear friend
Professor Boris Malkin on the occasion
of his 80th anniversary*

1. Introductory remarks

Lent with coworkers proposed a revolutionary concept to use cells composed of quantum dots [1–3] which are coupled via Coulomb interaction to form a cellular automata architecture. This concept gave rise to the intense development of the new multidisciplinary field of nanotechnology known as quantum dot cellular automata (QCA). The transistorless QCA devices opened new fascinating perspectives for computing because they consume much smaller amount of electrical power and exhibit negligible heat release as compared with the traditional devices based on field effect transistors. Due to these advantages of crucial significance, the QCA devices are of great potential importance to perform computations at very high switching rate.

The QCA have been realized as arrays of quantum-dot cells grafted on a silicon substrate. In search of more compact electronic devices which would enhance the advantages of QCA, later on the concept of molecular QCA has been proposed. Within this concept instead of quantum dots, the molecules with appropriate structures have been proposed as cells encoding binary information. The main attention has been paid to mixed valence (MV) metal clusters and organic molecules containing excessive electrons or holes [4–8]. Structural peculiarities of these compound and charge configurations allow use them as molecular cells. As distinguished from quantum-dot QCA, in molecular MV systems the redox sites play role of the charge containers. Each cell typically consists of four dots (or four redox centers in the case of molecular cell) situated in the vertices of a square and two extra electrons tunneling between the dots or redox centers. Use of the molecules instead of dots allows to significantly increase the density of cells grafted on the surface and hopefully to significantly decrease the heat release due to relatively weak coupling of molecules with the thermal bath.

2. Examples of logical gates

The binary information in QCA is encoded in the two diagonal (antipodal) localizations of the electronic pair within the square cell to minimize the Coulomb repulsion energy of the two electrons. These two localized configurations of the mobile charges correspond to the binary 1 and 0. The binary information is transmitted through the intercell Coulomb interaction, which is wireless and therefore, excludes the ohmic losses. This allows to compose different kinds of logical devices (such as wires, majority gates, etc.) on the basis of the two-electron square cells. In order to illustrate the typical compositions of QCA devices, in Figure 1 the two examples of the electronic components based on the molecular or quantum dot square cells are depicted. Fanout (Figure 1) bifurcates the signal (input 1 is transformed into two outputs 1), while the inverter inverts the signal (input 1 gives output 0). One can see that the required configurations of the constituent charges are organized by the requirement of the minimum of Coulomb repulsion energy within the cell architecture.

The theoretical consideration of the problem of QCA includes at least two steps: analysis of an isolated cell and consideration of the interacting cells. The first part of the problem is dealing with the electronic and vibronic interaction in an isolated square-planar MV molecule [9–14] and search of the optimal way to organize a cell (molecular or composed of quantum dots). The second part of the problem is the study of the influence of the driver on the working cell including static and dynamic polarization and thermalization processes.

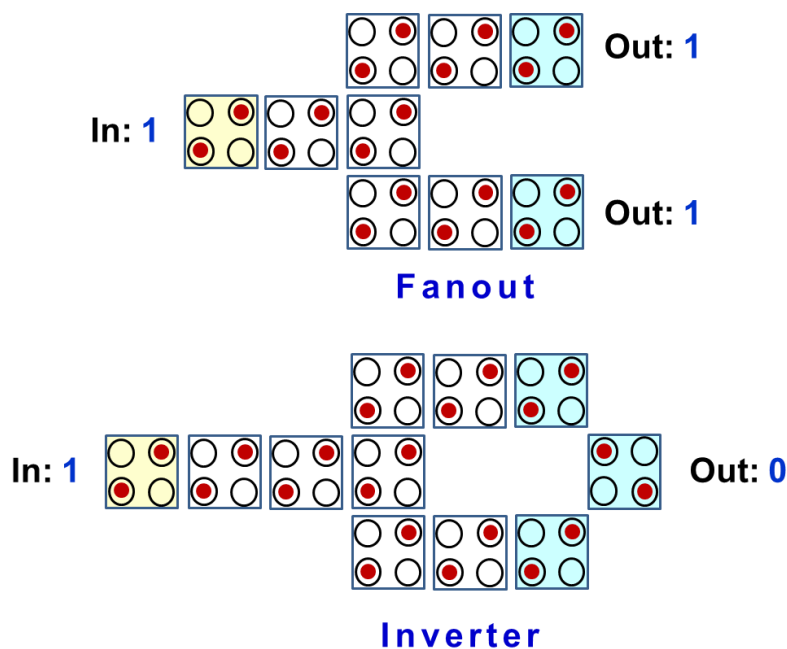


Figure 1. Schemes of fanout and inverter built from square cells. Filled balls denote charged sites.

3. The main issue of the present consideration

In this article we consider the problem of organization of the cell in molecular QCA and action of driver cell in the two important ways of the cell organization. The square cell can be composed in the two different ways. [15] The first way is to tailor two dimeric units, each containing single mobile electron. [4–6] The dimeric units in this case can be referred to as half-cells. In principle, experimentally this way to get a full cell can be realized by a proper deposition of the dimeric units on a surface and then to tailor logical gates and fabricate circuits. The present day state-of-art in this area allows to consider this technological task as a realistic one. The second way

is to use entire tetramer with two extra electrons as a full-cell. [7, 8] Hereunder we report the comparative theoretical analysis of the efficiencies of these two kinds of compositions of the square cells. For the sake of brevity in the consequent consideration the two kinds of cells will be referred to as “double-dimeric cell” and “tetrameric cell”. In this analysis we will focus on such important functional characteristic of QCA as the so-called “cell-cell response function”, which represents the dependence of the polarization of a definite cell on the polarization of the neighboring cell acting as driver. The necessary condition of the proper functionality of the QCA device is the fast response of the working cell on the small change of the polarization of the driver.

4. The model and the Hamiltonian

We adopt the model in which the isolated two-electron square cell is described by the following Hubbard-type Hamiltonian which includes electron transfer processes and Coulomb repulsion:

$$\hat{H}_c = \sum_{i<j} \left[U_{ij} n_{i,\sigma} n_{j,\sigma'} + \sum_{\sigma} t_{ij} \left(a_{i,\sigma}^{\dagger} a_{j,\sigma} + a_{j,\sigma}^{\dagger} a_{i,\sigma} \right) \right], \quad (1)$$

The first term in Eq. (1) describes the interelectronic Coulomb repulsion. For a square cell this interaction is defined by the following parameters:

$$U_{12} = U_{23} = U_{34} = U_{14} \equiv U_n, \quad U_{13} = U_{24} \equiv U_d, \quad (2)$$

where indexes n and d are introduced to distinguish between the Coulomb repulsion energies of two electrons occupying nearest (n) neighboring quantum dots (or redox sites) and those situated in the remote (along the diagonal (d)) positions in a square cell. The two diagonal dispositions (1, 3) and (2, 4) of the electronic pair in the square cell possess smaller Coulomb repulsion energies (ground Coulomb manifold) as compared with the four nearest neighboring dispositions (excited manifold), so that the Coulomb energy gap

$$U \equiv U_n - U_d \quad (3)$$

is always positive.

The second term in Eq. (1) describes the electron transfer between the different sites, where t_{ij} is the set of transfer parameters. The latter depends on the composition of the square cell as can be seen from Figure 2. We assume that the electron transfer processes only between the nearest neighboring sites are allowed. Thus, there are four transfer pathways in the tetrameric square cell, and so such cell is described by the following transfer parameter:

$$t_{12} = t_{23} = t_{34} = t_{14} \equiv t. \quad (4)$$

In the cell composed of two dimers 1-2 and 3-4 the transfer integrals t_{23} and t_{14} are vanishing, and hence only two transfer pathways are allowed:

$$t_{12} = t_{34} \equiv t. \quad (5)$$

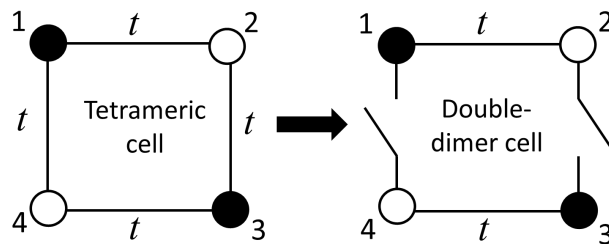


Figure 2. Illustration for the two possible compositions of the square cell with the indication of the allowed electron transfer pathways.

This means that although the two possible compositions of the square cell are equivalent from the point of view of the Coulomb repulsion between the two electrons, they are different from the point of view of the allowed transfer pathways.

The bi-electron eigenstates of the Hamiltonian, Eq. (1), can be subdivided into the spin-singlets and spin-triplets. In the case of double-dimeric cell all the eigenstates of the Hamiltonian, Eq. (1), are degenerate with respect to the spin of the cell. In contrast, in the case of tetrameric cell the energies of the cell are spin-dependent, and in the adopted model of transfer pathways neglecting the diagonal transfers the ground state of the cell is shown to be always a spin-singlet. More detailed analysis shows that the latter statement proves to be valid even if the cell is subjected to the action of the quadrupole Coulomb field of neighboring cell acting as a driver. For the sake of simplicity here we discuss the properties of QCA in the low-temperature limit when only the ground state is populated. For this reason, we exclusively focus on the spin-singlets.

5. The case of strong Coulomb repulsion, electronic densities

Now we will proceed to the most relevant case of $U \gg t$ in which the Coulomb repulsion competing with the transfer processes, is able to well separate the charges in the antipodal configurations. Under the condition of strong Coulomb repulsion one can project the initial cell Hamiltonian, Eq. (1), onto the restricted set of only two spin-singlet states (1, 3) and (2, 4), which form the ground manifold of the cell. Also, at this step along with the intracell interactions, we will take into account the interaction of a definite cell 1 – 2 – 3 – 4 (working cell) with the neighboring polarized square cell 1' – 2' – 3' – 4' acting as a driver which produces an external quadrupole Coulomb field. The mutual disposition of the two cells is shown in Figure 3. In this way we obtain the following effective second-order Hamiltonian of the working cell subjected to the action of the driver:

$$\hat{V}_c = -\frac{Nt^2}{U} (\hat{\sigma}_0 + \hat{\sigma}_x) - uP'\hat{\sigma}_z, \quad (6)$$

where $\hat{\sigma}_0$ is the unit 2×2 -matrix, $\hat{\sigma}_x$ and $\hat{\sigma}_z$ the Pauli matrices defined in the basis composed of the states (1, 3), (2, 4). The first term in Eq. (6) describes the isolated cell and represents the projection of the initial Hamiltonian, Eq. (1), onto the ground Coulomb manifold. The factor N depends on the composition of the square cell. Thus, $N = 2$ for the double-dimeric cell and $N = 4$ for the tetrameric cell, that are just the number of allowed transfer pathways for different

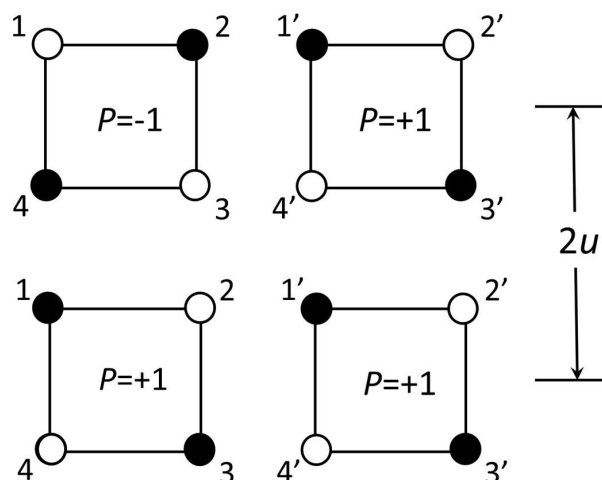


Figure 3. Mutual disposition of the two interacting cells and illustration of the maximal intercell Coulomb gap $2u$.

cell compositions. The second term describes the quadrupole-quadrupole pair of the Coulomb interaction between the definite cell 1–2–3–4 and the driver 1′–2′–3′–4′ with the prepared polarization P' . This polarization is defined as follows:

$$P' = \frac{\rho_{1'3'} - \rho_{2'4'}}{\rho_{1'3'} + \rho_{2'4'}}, \quad (7)$$

where $\rho_{1'3'}$ and $\rho_{2'4'}$ are the probabilities (normalized electronic densities) in the two diagonal localizations of the electronic pair ($\rho_{1'3'} + \rho_{2'4'} = 1$). It is assumed that polarization of the driver can be changed in a controllable manner in between two limits of full polarization $P' = -1$ ($\rho_{1'3'} = 0, \rho_{2'4'} = 1$) to $P' = +1$ ($\rho_{1'3'} = 1, \rho_{2'4'} = 0$). At $P' = 0$ the electronic densities are equally distributed between two diagonals ($\rho_{1'3'} = \rho_{2'4'} = 1/2$). When the driver is polarized, it induces the polarization on a working cell 1–2–3–4. The polarization P is defined by Eq. (7) in which one should make substitutions $\rho_{1'3'} \rightarrow \rho_{13}, \rho_{2'4'} \rightarrow \rho_{24}$ and $P' \rightarrow P$. The parameter u describes the intercell Coulomb interaction. To clarify the physical meaning of this parameter let us note that at $t = 0$ the eigenvalues of \hat{V}_c are linearly dependent on the polarization P' of the driver:

$$E_{(1,3)}(P') = -P'u, \quad E_{(2,4)}(P') = P'u. \quad (8)$$

It thus follows from Eq. (7) that the gap $2u$ can be represented as:

$$2u = E_{(2,4)}(P' = 1) - E_{(1,3)}(P' = 1). \quad (9)$$

Hence the value $2u$ represents the maximal Coulomb gap between the energies corresponding to the two different distributions of four electrons within the two interacting cells. In fact, the Coulomb energy for $P = \mp 1$ and $P' = \pm 1$ corresponds to maximal possible Coulomb energy of the two fully polarized cells which corresponds to extremely energetically unfavorable four-electron Coulomb configuration, while the energy for $P = \pm 1$ and $P' = \pm 1$ corresponds to the minimal Coulomb energy. This is illustrated in Figure 3 in which the mutual dispositions of the cells are shown along with their polarizations. The parameter u is therefore the function of the intracell and intercell distances, and also depends on the dielectric constant of the material for the dots deposited on the surface or also on the structure of the ligands in the case of MV compounds.

6. Cell-cell response function

To illustrate the main results in the framework of the Hubbard type model we plot the cell-cell response function $P(P')$ with the set of typical for molecular systems parameters. The knowledge of the eigenvectors of the Hamiltonian, Eq. (6), allows evaluation of the dependence of polarization P induced in the cell 1–2–3–4 on the polarization P' of a driver 1′–2′–3′–4′ that is just the cell-cell response function. Figure 4 shows the plots of $P(P')$ dependences for two possible compositions of square cell evaluated with the values $t^2/U = 30 \text{ cm}^{-1}$, $u = 250 \text{ cm}^{-1}$ which fall within the typical range of parameters for QCA. One can see that the steepness (non-linearity) is more pronounced for the double-dimeric cell.

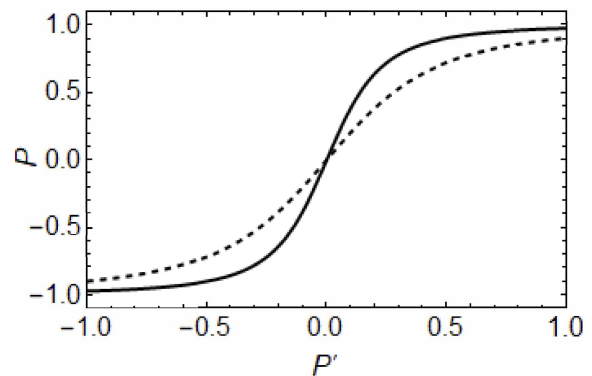


Figure 4. Comparison of the cell-cell response functions for the double dimeric (solid line) and tetrameric (dashed line) cells calculated with $t^2/U = 30 \text{ cm}^{-1}$ and $u = 250 \text{ cm}^{-1}$.

7. Qualitative remarks about the role of the vibronic coupling

The vibronic coupling plays an essential role in MV systems giving rise to the self-trapping effect. The detailed consideration of the vibronic coupling in the bi-electronic cells is given in [9–13] in the framework of the semiclassical adiabatic approach and within a more precise quantum-mechanical theory as applied to the pseudo Jahn-Teller problem. In general, the vibronic coupling creates bistability of of MV system so that the localized electronic states are separated by a potential barrier. A schematic picture of the double-well adiabatic potential of the system is shown in Figure 5. Providing strong vibronic coupling (and strong Coulomb repulsion) the electronic pair is almost fully localized in the two antipodal positions that means that the transfer processes are strongly reduced. Providing moderate vibronic coupling the system is partially localized as schematically shown in Figure 5 which means that the electronic density is mostly concentrated on the one well but the second well of the potential energy is also partially populated. In terms of the vibronic trapping the difference between the two kinds of cells so far discussed can be qualitatively predicted. In fact, in tetrameric systems the degree of localization in the antipodal positions is lower as compared with that in the double-dimeric ones and therefore the former systems are more resistant against external field. The vibronic coupling tends to reduce the transfer parameters and consequently to minimize the difference of the double-dimeric and tetrameric clusters with respect to the efficiency of the action of the driver.

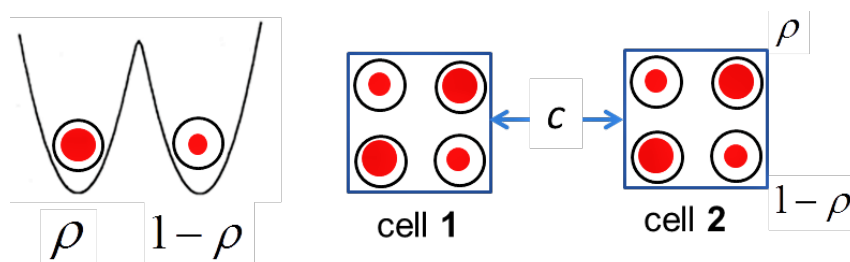


Figure 5. Schematic picture of the partial delocalization at the minima of a double-well adiabatic potential (left) and Coulombic cell-cell interaction resulting in the alignment of the two cells (right). Modified from Ref. [13].

8. Concluding remarks

It is seen (Figure 4) that the steepness of the non-linear $P(P')$ dependence is higher for the double dimeric cell. In addition, as distinguished from the double dimeric cell the polarization P of the tetrameric cell does not reach the saturation values ± 1 at $P' = \pm 1$. These differences in the cell-cell responses appear due to twice larger magnitude of effective second-order transfer parameter for the tetrameric cell and hence lower sensitivity of such to the quadrupole field induced by the driver. We thus arrive at the conclusion that the double-dimeric cell is more efficient for functioning of ACA as compared with the tetrameric cell. This means that providing identical geometries, transfer parameters and Coulomb repulsion the double-dimeric cell is more sensitive to the action of the driver. This conclusion seems to be useful for the controlled design of suitable cells in QCA architecture.

Acknowledgment

Support from the Ministry of Science and Higher Education of the Russian Federation (Agreement No. 14.W03.31.0001 Institute of Problems of Chemical Physics, Chernogolovka) is acknowledged.

References

1. Lent C.S., Tougaw P.D., Porod W., Bernstein G.H. *Nanotechnology* **4**, 49 (1993)
2. Tougaw P.D., Lent C.S. *J. Appl. Phys.* **75**, 1818 (1994)
3. Orlov A.O., Amlani I., Bernstein G.H., Lent C.S., Snider G.L. *Science* **277**, 928 (2003)
4. Lent C.S., Isaksen B., Lieberman J. *Am. Chem. Soc.* **125**, 1056 (2003)
5. Li Z., Beatty A.M., Fehner T.P. *Inorg. Chem.* **42**, 5707 (2003)
6. Qi H., Sharma S., Li Z., Snider G.L., Orlov A.O., Lent C.S., Fehner T.P. *J. Am. Chem. Soc.* **125**, 15250 (2003)
7. Jiao J., Long G.J., Rebbouh L., Grandjean F., Beatty A.M., Fehner T.P. *J. Am. Chem. Soc.* **127**, 17819 (2005)
8. Nemykin V.N., Rohde G.T., Barret C.D., Hadt R.G., Bizzarri C., Galloni P., Floris B., Nowik I., Herber R.H., Marrani A.G., Zanoni R. *J. Am. Chem. Soc.* **131**, 14969 (2009)
9. Tsukerblat B., Palii A., Clemente-Juan J.M. *Pure Appl. Chem.* **87(3)**, 271 (2015)
10. Tsukerblat B., Clemente-Juan J.M., Coronado E. *J. Chem. Phys.* **143**, 134307 (2015)
11. Clemente-Juan J.M., Palii A., Coronado E., Tsukerblat B. *J. Chem. Theory Comput.* **12** 3545 (2016)
12. Palii A., Tsukerblat B., Clemente-Juan J.M., Coronado E. *J. Phys. Chem.* **120**, 16994 (2016)
13. Tsukerblat B., Palii A., Clemente-Juan J.M., Suaud N., Coronado E. *Acta Phys. Polonica A* **133**, 329 (2018)
14. Palii A., Tsukerblat B. *Dalton Trans.* **45**, 16661 (2016)
15. Hennessy K., Lent C.S. *J. Vac. Sci. Technol. B: Microelectron Process. Phenom.* **19**, 1752 (2001)